ce/papers
The online collection for conference papers in civil engineering
Ernst & Sohn A Wiley Brand

ORIGINAL ARTICLE

eurosteel SHEFFIELD 2021
Ernst & Sohn A Wiley Brand

Numerical-experimental analysis of a braced steel frame subjected to fire following earthquake

Patrick Covi[1], Nicola Tondini[1], Manfred Korzen[2], Georgios Tsionis[3]

Correspondence

Dr. Nicola Tondini
University of Trento
Department of Civil, Environmental and Mechanical Engineering
via Mesiano 77
38123 Trento, Italy
Email: nicola.tondini@unitn.it

Affiliations

[1]University of Trento, Trento, Italy.
[2]Bundesanstalt für Materialforschung und –prüfung (BAM), Berlin, Germany.
[3]European Commission, Joint Research Centre, Ispra, Italy

Abstract

Many historical events have shown that, after an earthquake, fire may be triggered by seismic-induced rupture of gas piping, failure of electrical systems, etc. The current engineering design methods still ignores many aspects of multi-hazard and in particular fire following earthquake (FFE) analysis. In this respect, the aim of this paper is to study the behaviour of a braced steel frame subjected to seismic-induced fire. In particular, FFE numerical analyses were conducted on a four-storey three-bay braced steel frame with concentric bracings. The results of the numerical analyses served to design the FFE tests performed on unprotected and protected columns belonging to the bracing system. The fire tests after the seismic event were carried out by considering the effects of the surrounding seismically damaged structure. Results of the FFE tests on unprotected columns are reported along with the numerical model calibration.

Keywords

Multi-hazard analysis, fire following earthquake, concentrically braced steel frame, experimental tests

1 Introduction

Earthquakes are destructive and unpredictable events with catastrophic consequences for both people and built environment. Moreover, secondary triggered effects can strike further an already weakened community, i.e. ground shaking, surface faults, landslides and tsunamis. In this respect, also fires following earthquake (FFE) have historically produced large post-earthquake damage and losses in terms of lives, buildings and economic costs, like the San Francisco earthquake (1906), the Kobe earthquake (1995), the Turkey earthquake (2011), the Tohoku earthquake (2011) and the Christchurch earthquakes (2011). In detail, FFE are a considerable threat as they can be widespread both at the building level and at the regional level within the seismic affected area owing to the rupture of gas lines, failure of electrical systems etc. and at the same time failure of the compartmentation measures. Moreover, they are more difficult to tackle by the fire brigades because of their possible large number and extent as well as of possible disruptions within the infrastructural network that hinder their timely intervention and within the water supply system.

In this context, the structural fire performance can worsen significantly because the fire acts on an already damaged structure. Furthermore, passive and active fire protections may have also been damaged by the seismic action and the fire can spread more rapidly if compartmentation measures have failed. Thus, the seismic performance of the non-structural components may directly affect the fire performance of the structural members. As consequence, the minimization of the non-structural damage is paramount in mitigating the possible drop in structural fire performance. The loss of fire protection is particularly dangerous for steel structures because the high thermal conductivity associated with small profile thicknesses entails quick temperature rise in the profiles with consequent fast loss of strength and stiffness. Most of the literature involve numerical simulations on steel moment resisting frames [1][2][3][4] and only a few of them are dedicated to buckling-restrained and conventional brace systems [5][6]. Both developed a framework for evaluating the post-earthquake performance of steel structures in a multi-hazard context that incorporates tools that are capable of probabilistic structural analyses under fire and seismic loads. Experimental studies have been performed on single elements [7], beam-concrete joints made of filled steel tubes [8], and full-scale reinforced concrete frames [9][10]. The study of literature reveals that several numerical studies on the post-earthquake fire behaviour of structural components have been carried out without being supported by comprehensive experimental research. Moreover, works on non-structural components are also very limited. On these premises the European project called EQUFIRE was funded.

2 SERA EQUFIRE project

The EQUFIRE project aims to provide experimental data to investigate the post-earthquake fire performance of steel structures. It is part of the Transnational Access activities of the SERA project (www.sera-eu.org) at the ELSA Reaction Wall of the European Commission - Joint Research Centre (JRC). The project focuses on the analysis of the behaviour of a braced steel structure subjected to FFE through full-scale tests based on hybrid simulation at the ELSA

Reaction Wall and through tests on single elements at the furnace of the Federal Institute for Materials Research and Testing (BAM).

3 Case study

3.1 Design of the prototype building

A four-storey three-bay steel structure with concentric bracings in the central bay was selected as case study for simulations and experimental tests, as shown in Figure 1. This frame is part of an office building with a square plan (12.5 m x 12.5 m) and the location of the building was assumed to be in the city of Lisbon (Portugal); thus, in an area of medium-high seismicity. The interstorey height is 3.0 m except for the height of the first floor, which is equal to 3.6 m. The lateral force resisting system consists of concentrically braced frames (CBF). Figure 1 also shows the member sizes and the column that was then heated after the seismic event, i.e. the column represented in red. Due to experimental constraints, only one member was heated at BAM, whereas the whole first floor was built at the JRC.

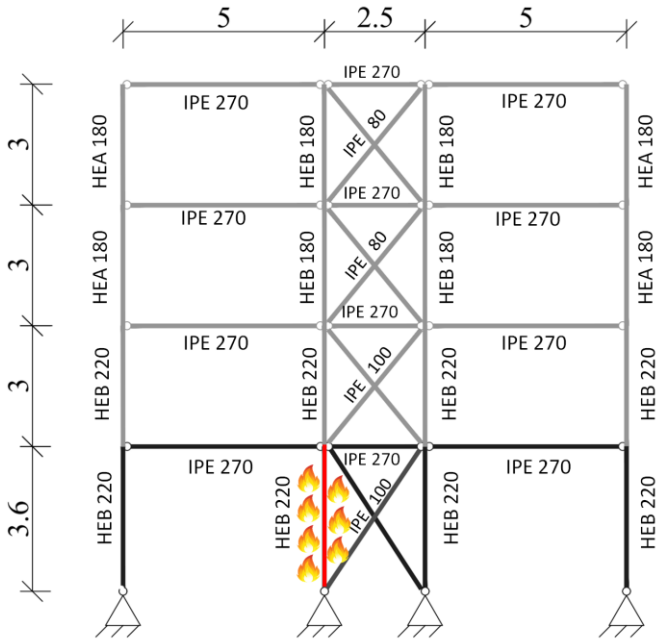

Figure 1 Test frame. Dimensions are in meters.

Two different steel grades were used, namely S275 and S355 (EN 10025-2, 2019). Steel grade S275 was adopted for the dissipative elements, i.e. the bracings, while steel grade S355 was selected for the non-dissipative members, i.e. columns, beams and connections. It is worth to point out that the yield strength for the bracings was taken as the mean value, i.e. 330 MPa, considering a coefficient of variation equal to 0.12, whereas for the non-dissipative members was taken the experimental value obtained through material testing, i.e. 436 MPa.

In detail, IPE sections with the weak axis in the plane of the frame were used for the bracing elements to force in-plane buckling for essentially two reasons: i) to avoid damage in the walls where the bracing is inserted in; ii) to keep a 2D modelling of the frame representative so that to maintain low computational demand for the hybrid tests.

In accordance with the Eurocode 8 [11], the frame was designed according to the capacity design criterion by employing a response-spectrum analysis (RSA). In particular, a "High Ductility Class (DCH)" was employed with dissipation in the bracing members. Then, non-linear time-history analyses with natural accelerograms were employed to investigate the seismic response of the structure. The general assumptions were the following:

- The columns were considered continuous along the height of the structure.
- All connections were assumed as pinned.
- The building was regular in plan and in elevation.
- The building was located in Lisbon characterised by peak ground acceleration equal to 0.186g and type B soil.

3.2 Set of accelerograms

In order to perform non-linear time-history analyses, it was fundamental to model the seismic hazard through adequate selection and scaling of ground motion records. In this respect, a set of fifteen accelerograms for the SD limit state was selected considering the type of spectrum, magnitude range, distance range, style-of-faulting, local site conditions, period range, and ground motion components using the INGV/EPOS/ORFEUS European Strong motion Database [12]. As shown in Figure 2, accelerograms were modified to match the target spectrum in the period range of 0.4÷0.9s that includes the fundamental period of the structure, i.e. 0.67 s. The accelerograms were used to perform nonlinear time-history analyses and fire following earthquake (FFE) analyses. A 2D and 3D model of the building was developed in OpenSees [13] software to conduct seismic, fire and FFE numerical analyses of the braced steel frame.

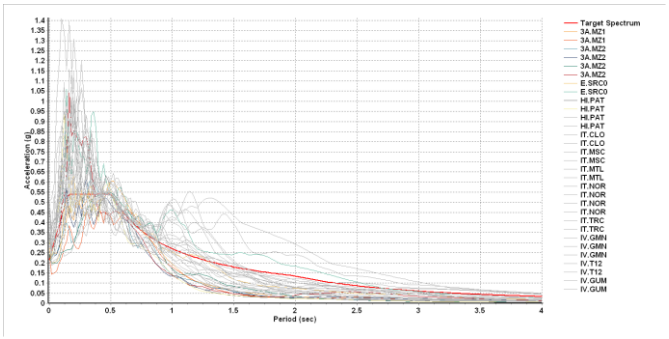

Figure 2 Comparison of the response spectra for original and modified vs the target spectrum.

The accelerogram shown in Figure 3 was selected for the experimental hybrid tests and the numerical analyses, based on three main requirements:

- The selected accelerogram had to cause significant damage to the bracings.
- The horizontal displacement of the first floor had to be equal or lower than ± 30 mm to be compatible with the horizontal actuator stroke of the BAM furnace.
- The axial force of the internal columns at the beginning of the second floor had to be below 1000 kN to be compatible with the actuators used to impose the vertical loads on the specimen at the ELSA Reaction Wall.

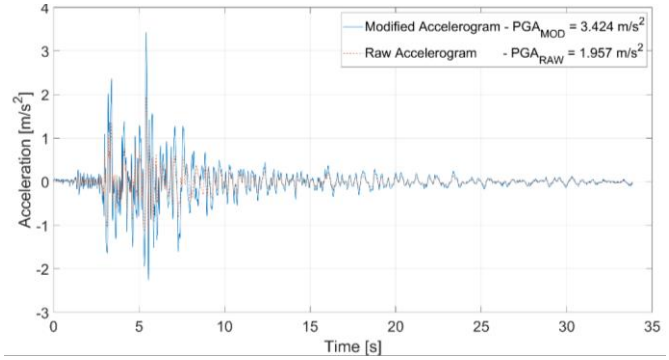

Figure 3 Selected accelerogram for simulations and tests.

4 Numerical simulations

4.1 Finite element model

A non-linear finite element model in OpenSees was developed to evaluate the FFE response of the structure, which is expected to experience large plastic deformations in the bracing elements due to the seismic action and in the column due to the fire exposure.

The fibre displacement-based beam-column element was used to model the beams, columns and braces. Seven non-linear beam elements based on corotational formulation and the uniaxial Giuffre-Menegotto-Pinto steel material, with isotropic strain hardening (Steel02Material) [16] and geometric nonlinearities was used for the bracing diagonals. Non-linear beam elements were used for all elements to check that non-dissipative elements remain in the elastic field owing to the seismic action. Geometric imperfections were included to allow for buckling EN 1993-1-1 [14]. Masses were considered lumped the floors, following the assumption of rigid diaphragms. The constitutive law provided by EN 1993-1-2 [15] was adopted to model the mechanical properties of steel at elevated temperature when for the column that was heated after the earthquake.

4.2 Fire following earthquake simulation

Figure 4 illustrates the results of the numerical simulation of the FFE test on the bare structure (without fire protection) for the selected acceleration time-history followed by the ISO 834 [17] heating curve. As is possible to observe, the energy dissipation is concentrated in the braces and in particular at the ground floor. The internal columns and all the other elements remained in the elastic field during the seismic event. After the earthquake, fire was initiated and collapse occurred 24 minutes after the start of the fire. Figure 4 also shows the final deformed configuration of the steel frame at the end of the simulation.

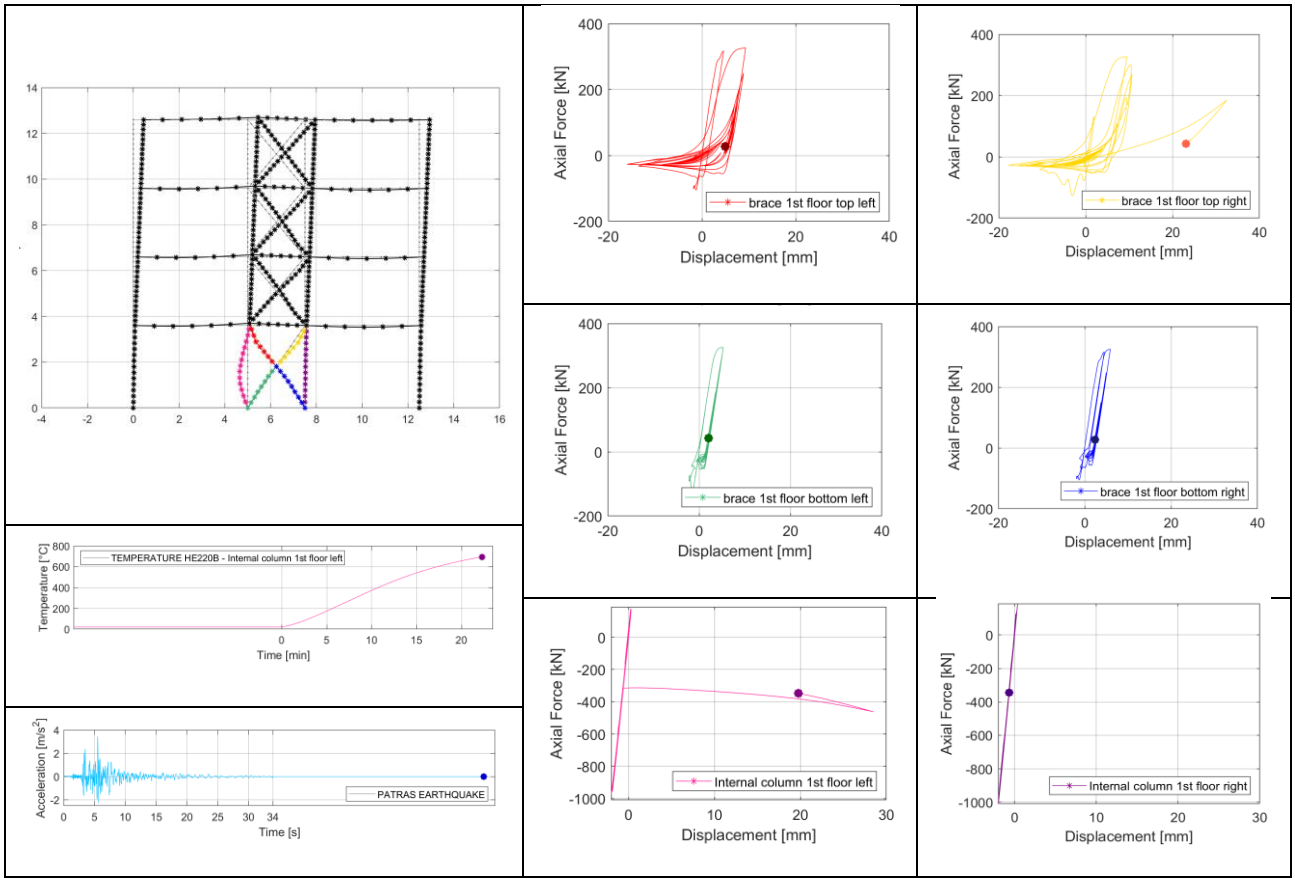

Figure 4 Numerical fire following earthquake simulation using OpenSees.

5 FFE tests at BAM

5.1 Experimental setup

The experimental tests at BAM were performed using a sub-structuring technique as shown in Figure 5, in which the physical column was firstly subjected to the horizontal and vertical displacement time-histories computed through numerical modelling (see Section 4). Then, the column was heated by the ISO 834 standard heating curve and a constant numerical axial stiffness representative of the surrounding structure was applied as boundary condition at the top of the physical column.

During the fire part of the FFE tests, the axial force of the column was measured and displacements were then imposed on the column in order to keep the two substructures in mechanical equilibrium.

Five FFE tests were conducted at BAM:

- Test #0 Column E: without fire protection system;
- Test #1 Column A: without fire protection system;
- Test #2 Column B: fire protection system, PROMATECT-H, designed for seismic region;
- Test #3 Column C: fire protection system, PROMATECT-H, not designed for seismic region;
- Test #4 Column D: sprayed vermiculite-type fire protection, designed for applications in seismic region". The mechanical reinforcing mesh retained the sprayed coating. It was located in the middle of the overall coating thickness.

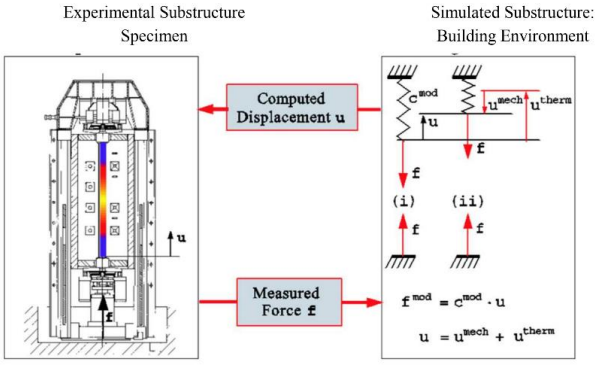

Figure 5 Sub-structuring method [18].

5.2 Equivalent stiffness of the numerical substructure during the fire events

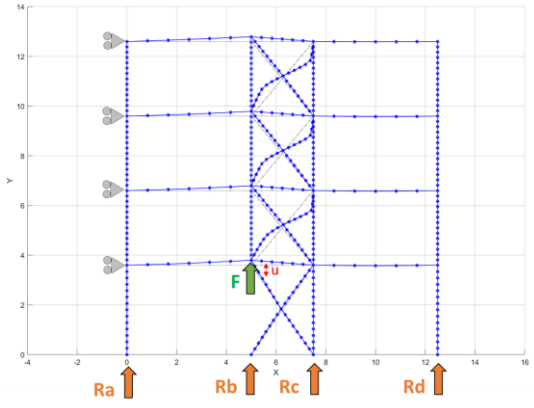

Figure 6 Static non-linear analysis to determine the axial stiffness value of the surrounding structure.

The axial stiffness of the upper part of the structure was numerically estimated by a static non-linear analysis. In detail, the full structure was subjected to gravity loads and to the selected accelerogram thorugh non-linear time-history analysis. Then the physical column was removed and the frame was constrained at each floor to reproduce the boundary condition of the actual experimental setup at BAM. Finally, a monotonic displacement-controlled pattern, which continuously increases, was performed, as depicted in Figure 6. As shown in Figure 7 the equivalent stiffness of the surrounding structure after the seismic event is neither constant nor linear. Due to this reason, it was not possible to exactly reproduce the same axial force condition in the column during the test. However, the value of K was chosen to reach a similar critical temperature.

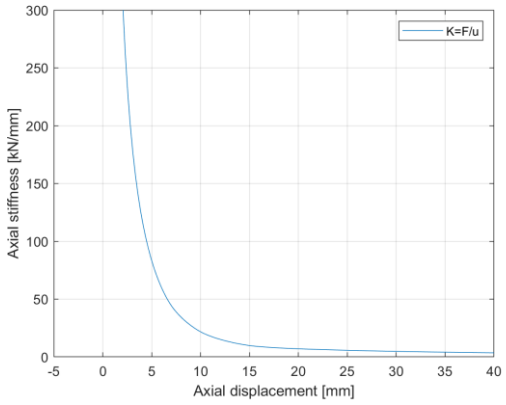

Figure 7 Axial stiffness of the surrounding structure vs axial displacement curve

In this respect, two 3D models of the physical specimen were modelled in OpenSees with two different boundary conditions on top, i.e. pinned (Case A) and fixed conditions (Case B). The column was modelled with 15 non-linear thermomechanical beam elements. It was first subjected to the gravity load, then to horizontal and vertical displacement histories resulting from seismic non-linear dynamic analysis. Afterwards, thermal action was applied with different constant axial stiffness values (K between 5 and 15 kN/mm) representative of the surrounding structure, as boundary conditions.

In order to determine the more appropriate equivalent axial stiffness value, Figure 8 shows the results in terms of the axial force and vertical displacement compared with the numerical analysis conducted on the whole structure. As it is possible to observe, a good value of the equivalent stiffness of the surrounding structure after the damage caused by the earthquake was equal to 5.3 kN/mm and this value was used in the tests. Moreover, the case with fixed conditions at the top of the column better agreed with the outcomes of the reference solution.

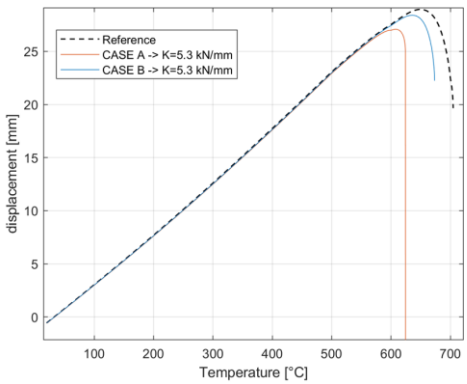

(a)

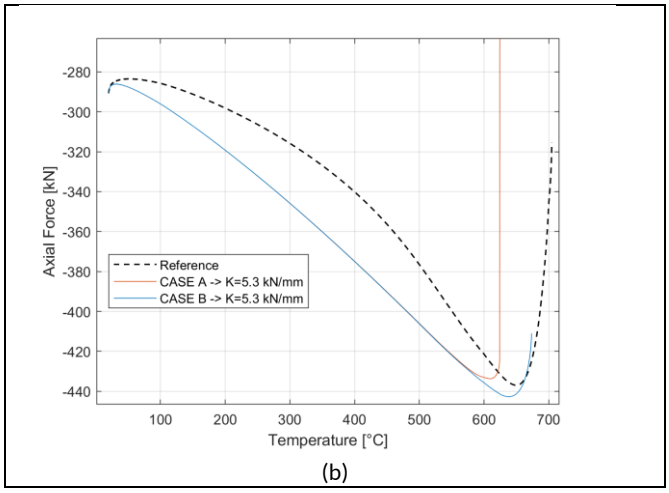

Figure 8 Comparison between the reference numerical solution and the single column with constant axial stiffness: a) axial displacements vs temperature curve; b) axial forces vs temperature curve.

6 Tests results

For brevity, only Test#0 and Test#1 are described in the following. The response history of the unprotected steel frame computed with OpenSees was compared against the results of the experimental tests at BAM. These results will be used for further calibration of the numerical model and for comparison with successive hybrid tests at JRC.

Figure 9 shows the axial displacement imposed to the specimens and the recorded axial force from the load cell. Overall the agreement is good. However, it is possible to observe that, due to the fairly high axial stiffness of the column, the actuator was not able to exactly follow the displacement time history and this implied some discrepancies in the applied force.

However, at the end of the seismic event, the recorded axial force was consistent with the one obtained through numerical simulation.

As expected, in all tests the columns remained in the elastic range being non-dissipative elements of the bracing system.

Figure 10 shows the results of the fire tests after the seismic event, for the two unprotected columns, i.e. Test #0 Column E and Test #1 Column A. The mean temperature in the cross section as well as the experimental axial displacement and the axial force are reported in Figure 10. Moreover, the comparison with the numerical model is also shown. Good agreement between the experimental outcomes and the numerical prediction obtained from model the whole frame can be observed for the first 23 min, time at which the numerical model experienced failure. Nonetheless, the experimental tests did not exhibit failure for the first 60 min. Thus, a calibration procedure of the numerical model was performed. It is worth pointing out that since the column was designed according to the capacity design, the utilisation factor in the fire situation was quite low and equal to 0.15.

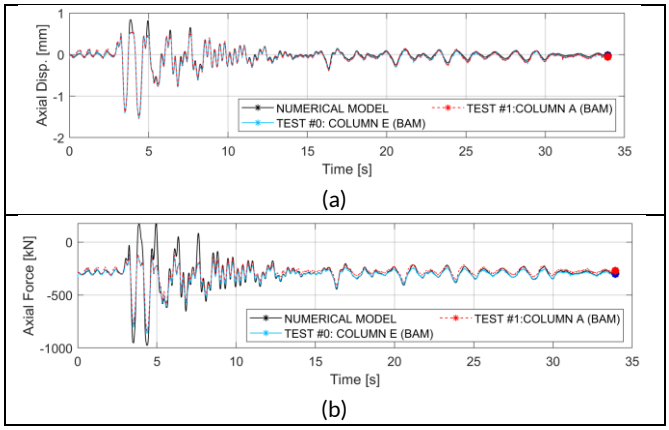

Figure 9 Seismic test: Comparison between the numerical solution and the tests: a) axial displacement and b) axial force.

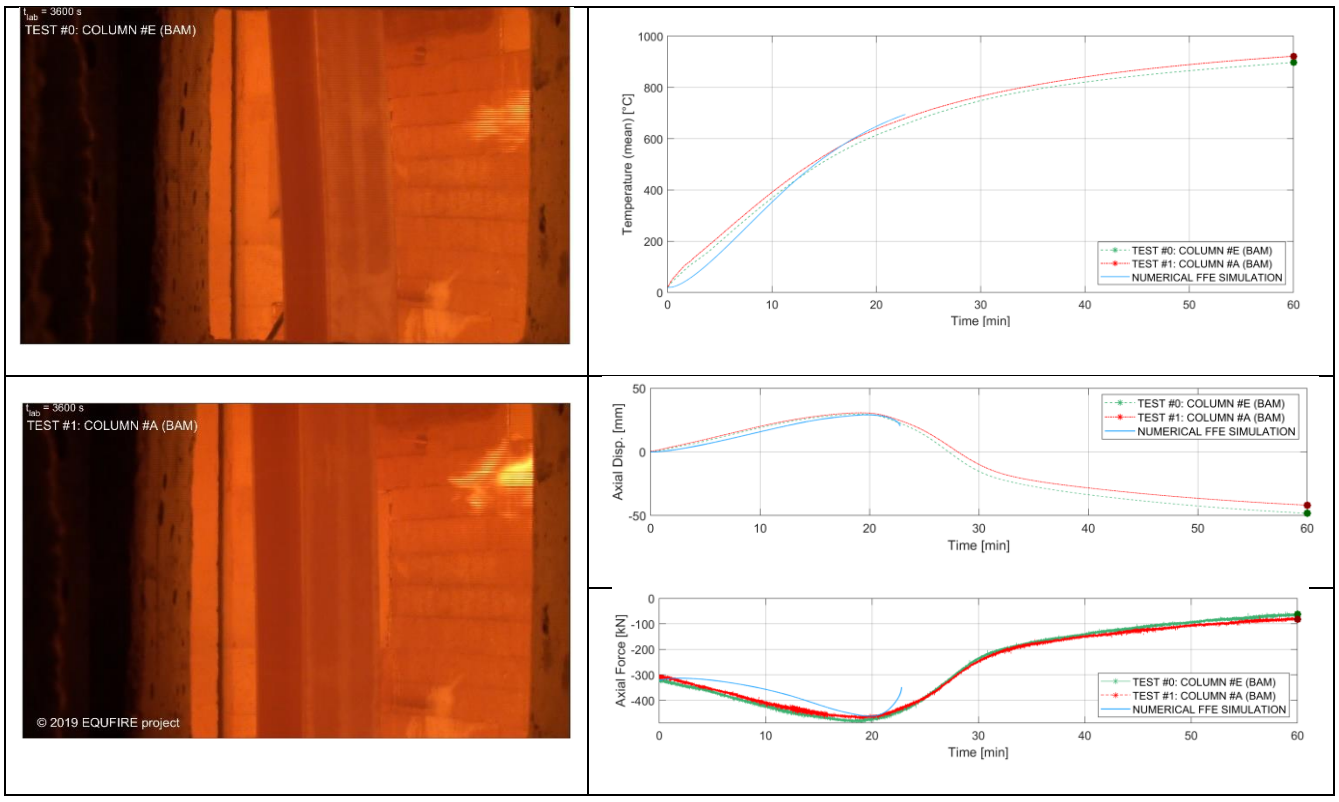

Figure 10 Comparison between the results of the numerical model and the FFE tests on the unprotected columns.

7 Model calibration

The calibration of the column numerical model consisted in modelling the boundary conditions by estimating the actual initial rotational stiffness based on the type of joint, as shown in Figure 11. In fact, the preliminary numerical analyses were carried out with pinned connections at the bottom end. However, the actual bottom end joint was not a nominal pin but instead it was made of a steel plate welded at the column and bolted to the base of the furnace. Therefore, even if the bolts were arranged in such a way to minimise the lever arm, some bending forces will always develop. For this reason, in the calibrated model the column was considered rotationally restrained at both ends using rotational springs that reproduce as close as possible the actual stiffness of the joints, as shown in Figure 12. The rotational stiffness K_{rot} of the base connection was numerically estimated by using a 3D finite element model of the joint and the estimated value was equal to 3.1 MNm/rad. In order to simplify, the same value of rotational stiffness was given at the top end too because the joint was similar. Moreover, for each specimen the recorded temperature evolution in the column along its height was applied in order to be more representative of the actual temperature distribution, as illustrated in Figure 12. The column was modelled with 3D thermomechanical beam elements. Geometric imperfections were included, whereas the residual stresses were neglected. The results of the model calibration are shown in Figure 13, in which it is possible to observe that a better agreement with experimental data, especially for the axial force, was achieved. Nevertheless, the numerical model reached failure after 28 min. This discrepancy may be caused by a temperature gradient within the cross-section, that was not considered in the modelling and by the actual rotational stiffness at the boundary conditions, that might have varied as fire test progressed. Indeed, since the column ends were protected, as shown in Figure 11, an increase in rotational stiffness offered by the joint relatively to the hot column as the steel temperature increased can be expected. Thus, a decrease of effective length could occur and this phenomenon was not taken into account because the rotational stiffness was kept constant during the simulation. In this respect, more refined numerical analyses are being performed.

Figure 11 End plate steel column connection.

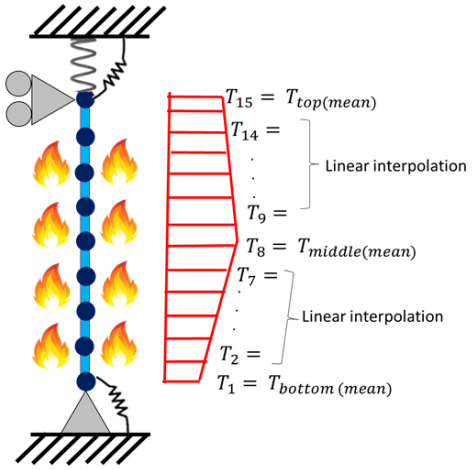

Figure 12 Calibrated numerical model: boundary conditions and temperature evolution along its height

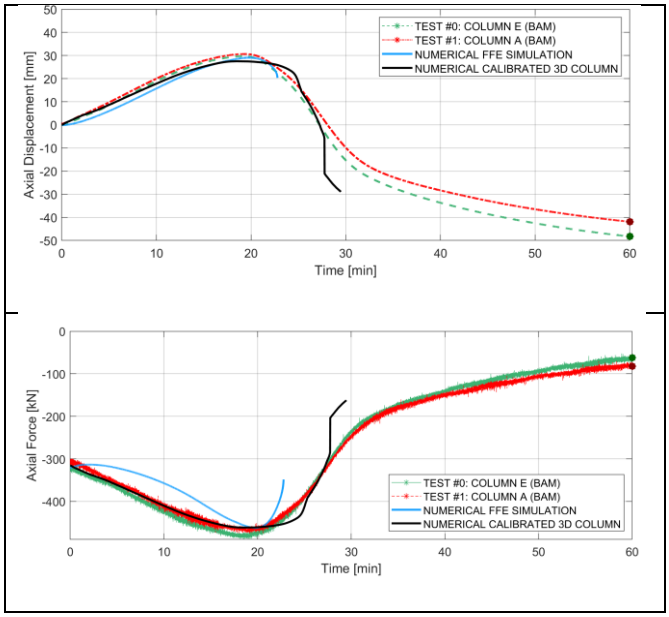

Figure 13 Comparison between the results of the numerical model, the calibrated 3D column and the FFE tests on the unprotected columns.

8 Conclusion

The paper presented part of the results of an experimental and numerical FFE analysis on a braced steel frame and in particular on columns belonging to the bracing system. The research activity was performed within the European EQUFIRE project. The numerical model developed in OpenSees was able to perform highly non-linear multi-hazard analyses and it served to design the FFE tests. As for the unprotected column tests, the specimens, as expected, remained in the elastic range after the seismic event at the Significant Damage limit state. During the successive fire tests performed by considering the effects of the surrounding structure through a constant axial stiffness, no failure was detected after 60 min of exposure to the ISO 834 heating curve. The main reason was the low utilisation factor in the fire situation. Model calibration was performed with beam finite elements that exhibited good agreement but also failure. This latter discrepancy may be caused by a temperature gradient within the cross-section, that was not considered in the modelling and by the actual rotational stiffness at the boundary conditions, that might have varied as fire test progressed. Thus, among the future perspectives there will be an activity related to a more refined numerical modelling.

Acknowledgements

This project has received funding from the European Union's Horizon 2020 Research and Innovation Programme, under grant agreement No. 730900. Authors would also acknowledge Philippe Buchet (EC-JRC) as well as Sven Riemer (BAM) Kai-Uwe Ziener (BAM), Marco Antonelli and Peter Schultz (ETEX-PROMAT) for their invaluable contribution to the experimental campaign.

References

[1] Della Corte G, Landolfo R, Mazzolani, FM. Post earthquake fire resistance of moment resisting steel frames, Fire Safety Journal, Vol. 38, No. 7, pp. 593-612, 2003.

[2] Memari M, Mahmoud M, Ellingwood B. Post-earthquake fire performance of moment resisting frames with reduced beam section connections, Journal of Constructional Steel Research, 103:215–229, 2014.

[3] Behnam B, Ronagh HR. Post-Earthquake Fire Performance-based Behavior of Unprotected Moment Resisting 2D Steel Frames, KSCE Journal of Civil Engineering 19(1):274-284, 2015.

[4] Keller WJ, Pessiki SP. Effect of earthquake-induced damage to spray-applied fire-resistive insulation on the response of steel moment-frame beam-column connections during fire exposure, Journal of Fire Protection Engineering 22(4) 271–299, 2012.

[5] Talebi E., Tahir M., Zahmatkesh F., Kueh A., Said A. Fire Resistance of a Damaged Building Employing Buckling Restrained Braced System (2017). International Journal of Advanced Steel Construction. In Press.

[6] Khorasani NE, Garlock MEM, Quiel SE. Modeling steel structures in OpenSees: Enhancements for fire and multi-hazard probabilistic analyses, Computers and Structures, 157:218–231, 2015.

[7] Braxtan NL, Pessiki SP. Postearthquake Fire Performance of Sprayed Fire-Resistive Material on Steel Moment Frames, Journal of Structural Engineering, 137(9): 946-953, 2011.

[8] Pucinotti R, Bursi OS, Demonceau JF. Post-earthquake fire and seismic performance of welded steel–concrete composite beam-to-column joints, Journal of Constructional Steel Research, 67:1358–1375, 2011.

[9] Kamath P, Sharma UK, Kumar V, Bhargava P, Usmani A, Singh B, Singh Y, Torero J, Gillie M, Pankaj P. Full-scale fire test on an earthquake-damaged reinforced concrete frame, Fire Safety Journal, 73:1–19, 2015.

[10] Meacham BJ. Post-Earthquake Fire Performance of Buildings: Summary of a Large-Scale Experiment and Conceptual Framework for Integrated Performance-Based Seismic and Fire Design, Fire Technology, 52(4):1133–1157, 2016.

[11] CEN (2005): EN 1993-1-2 Eurocode 3: Design of steel structures - Part 1-2: General rules - Structural fire design.

[12] Luzi L, Puglia R, Russo E & ORFEUS WG5 (2016). Engineering Strong Motion Database, version 1.0. Istituto Nazionale di Geofisica e Vulcanologia, Observatories & Research Facilities for European Seismology. doi: 10.13127/ESM.

[13] McKenna F., (2011) “OpenSees: A Framework for Earthquake Engineering Simulation”, Computing in Science and Engineering.

[14] CEN (2005): EN 1993-1-1 Eurocode 3: Design of steel structures - Part 1-1: General rules and rules for buildings.

[15] CEN (2005): EN 1993-1-2 Eurocode 3: Design of steel structures - Part 1-2: General rules - Structural fire design.

[16] Silva, V., Crowley, H., Varum, H. et al. (2015): “Seismic risk assessment for mainland Portugal” Bull Earthquake Eng 13: 429.

[17] ISO (1999): ISO834-1:1999, Fire-resistance tests -Elements of building construction- Part 1: General requirements.

[18] Korzen, M., Magonette, G., Buchet, P. (1999) “Mechanical loading of columns in fire tests by means of the substructuring method”, 8th, INTERFLAM '99: Fire science and engineering conference.